

## Accepted Manuscript

Title: Determination of ACIDITY constants and prediction of electrophoretic separation of amyloid Beta peptides

Authors: Roger Peró-Gascón, Fernando Benavente, José Barbosa, Victoria Sanz-Nebot



PII: S0021-9673(17)30829-4  
DOI: <http://dx.doi.org/doi:10.1016/j.chroma.2017.05.069>  
Reference: CHROMA 358566

To appear in: *Journal of Chromatography A*

Received date: 15-3-2017  
Revised date: 16-5-2017  
Accepted date: 31-5-2017

Please cite this article as: Roger Peró-Gascón, Fernando Benavente, José Barbosa, Victoria Sanz-Nebot, Determination of ACIDITY constants and prediction of electrophoretic separation of amyloid Beta peptides, *Journal of Chromatography A* <http://dx.doi.org/10.1016/j.chroma.2017.05.069>

This is a PDF file of an unedited manuscript that has been accepted for publication. As a service to our customers we are providing this early version of the manuscript. The manuscript will undergo copyediting, typesetting, and review of the resulting proof before it is published in its final form. Please note that during the production process errors may be discovered which could affect the content, and all legal disclaimers that apply to the journal pertain.

# DETERMINATION OF ACIDITY CONSTANTS AND PREDICTION OF ELECTROPHORETIC SEPARATION OF AMYLOID BETA PEPTIDES.

Roger Peró-Gascón, Fernando Benavente, José Barbosa, Victoria Sanz-Nebot\*

Department of Chemical Engineering and Analytical Chemistry, University of Barcelona, c/ Martí i Franqués 1-11, 3rd floor, 08028 Barcelona, Spain

\*Corresponding author: vsanz@ub.edu (V. Sanz-Nebot, PhD)

Tel: (+34) 934021283, Fax: (+34) 934021233

## Highlights

- A strategy to estimate the  $pK_a$  values of complex polyprotic peptides is described.
- The  $pK_a$  values of 5 fragments of A $\beta$  peptides 1-40 and 1-42 are determined by CE-UV.
- $pK_a$  accuracy is demonstrated validating the polymer model ( $m_e \propto q/M_r^{1/2}$ ).
- Separations are predicted for A $\beta$  peptides 1-40 and 1-42, or their fragments.
- pH and EOF are considered in selectivity and electropherogram predictions.

## ABSTRACT

In this paper we describe a strategy to estimate by CE the acidity constants ( $pK_a$ ) of complex polyprotic peptides from their building peptide fragments. CE has been used for the determination of the  $pK_a$ s of five short polyprotic peptides that cover all the sequence of amyloid beta (A $\beta$ ) peptides 1-40 and 1-42 (A $\beta$  fragments 1-15, 10-20, 20-29, 25-35 and 33-42). First, the electrophoretic mobility ( $m_e$ ) was measured as a function of pH of the background electrolyte (BGE) in the pH range 2-12 (bare fused silica capillary, I=25mM and T=25°C). Second, the  $m_e$ s were fitted to equations

modelling the ionisable behaviour of the different fragments as a function of pH to determine their  $pK_{as}$ . The accuracy of the  $pK_{as}$  was demonstrated predicting the electrophoretic behaviour of the studied fragments using the classical semiempirical relationships between  $m_e$  and peptide charge-to-mass ratio ( $m_e$  vs.  $q/M_r^{1/2}$ , classical polymer model,  $q$ =charge and  $M_r$ =relative molecular mass). Separation selectivity in a mixture of the fragments as a function of pH was evaluated, taking into account the influence of the EOF at each pH value, and a method for the simple and rapid simulation of the electropherograms at the optimum separation pH was described. Finally, the  $pK_{as}$  of the fragments were used to estimate the  $pK_{as}$  of the A $\beta$  peptides 1-40 and 1-42 ( $^1C$  and D 3.1, E 4.6 and Y 10.8 for acidic amino acids and  $^1N$ -D 8.6, H 6.0, K 10.6 and R 12.5 for basic amino acids), which were used to predict their behaviour and simulate their electropherograms with excellent results. However, as expected due to the very small differences on  $q/M_r^{1/2}$  values, separation resolution of their mixtures was poor over the whole pH range. The use of poly(vinyl alcohol) (PVA) coated capillaries allowed reducing the electroosmotic flow (EOF) and a slight improvement of resolution.

**KEYWORDS:** Acid dissociation constant / Amyloid beta / Capillary electrophoresis / Peptides /  $pK_a$  / Prediction

## **1. Introduction**

The acid dissociation constant ( $K_a$ , or  $pK_a$  in minus logarithm scale) is a fundamental parameter for physicochemical characterization of biologically and pharmacologically relevant compounds [1,2]. Capillary electrophoresis (CE) has been widely used for

accurate determination of  $pK_a$  of a great variety of polyprotic compounds [1–4]. It is an excellent alternative to potentiometric [2,5], ultraviolet-visible (UV/Vis) spectrophotometric [2,6] and NMR [2,7] determination because it is not limited by sample volume or purity, it can be fully automated and it allows a great versatility in the selection of the separation conditions. The CE determination of  $pK_a$  is usually performed measuring the electrophoretic mobility ( $m_e$ ) of the target compounds as a function of pH within an appropriate pH range in aqueous solutions [4], mixed hydro-organic [8] or non-aqueous media [9] using fused silica capillaries with UV detection [4,8,9]. During the last decade, different interesting alternatives have been proposed to increase the reproducibility and throughput of these typical procedures, such as application of multiplexed [10] and miniaturized instrumentation [11], coated capillaries [12,13], mass spectrometry detection [14,15] or internal standard-based methods [16]. However, most of the applications have been described for small molecules with only a few ionisable groups (less than 4). The determination of  $pK_{a,s}$  is troublesome for polyprotic compounds with many ionisable groups, especially when expected  $pK_{a,s}$  are extreme or correspond to the same or similar ionisable groups. This is the case of proteins and polypeptides, which may have dozens of  $pK_{a,s}$ . An interesting approach to estimate the  $pK_{a,s}$  of polypeptides may be the study of several fragment peptides with a smaller number of ionisable groups to cover the complete parent sequence. Following a similar strategy, Rickard et al. reported an excellent general set of average  $pK_a$  values for amino acids in polypeptides using biosynthetic human insulin (BHI) and human growth hormone (hGH) short fragments with a few ionisable groups [17].

The development of rapid, efficient and high-resolution separations in CE requires a previous optimisation. This optimisation can be assisted by modelling the

electrophoretic behaviour of the target compounds to avoid excessive experimental work [15,18–21]. Accurate quantitative relationships between the  $m_e$  of ionisable compounds and the pH of the background electrolyte (BGE) have proved to be very useful to simultaneously determine their  $pK_{as}$  and the optimum pH for their separation in a complex mixture [15,18]. Moreover, several semiempirical relationships relating the  $m_e$  of the analytes to their structure (charge, molecular mass or number of amino acid residues) have been proposed [15,18–21]. In previous works, these classical semiempirical relationships yielded excellent correlations for several peptide hormones [15], neuropeptides [18], apothioneins [19], peptides and glycopeptides from tryptic digests of glycoproteins [20] and quinolones [21] when good estimates of  $pK_a$  values were available for charge calculations.

In this work, a general equation relating the  $m_e$  with pH,  $pK_{as}$  and activity coefficients is used to model the migration behavior and determine the  $pK_{as}$  of five amyloid beta ( $A\beta$ ) peptide fragments (1-15, 10-20, 20-29, 25-35 and 33-42) that cover all the sequence of  $A\beta$  peptides 1-40 and 1-42.  $A\beta$  1-40 and 1-42 are clinical biomarkers used for Alzheimer's disease diagnosis, which is nowadays one of the most common age-related neurodegenerative disorders [22,23].  $A\beta$  peptides are produced during normal cellular metabolism and are constituents of biological fluids but under pathological conditions they aggregate and form amyloidotic fibrils which are deposited and accumulated in the brain as plaques. As protein aggregation depends on pH [24,25], characterization of the physicochemical parameters of these peptides is important. Once the  $pK_{as}$  of the  $A\beta$  peptide fragments were determined by CE, the classical polymer model ( $m_e$  vs.  $q/M_r^{1/2}$ ,  $q$ =charge and  $M_r$ =relative molecular mass) was used to predict the separation of a mixture of the fragments and confirm the accuracy of the  $pK_{as}$ .

Finally, we demonstrated that the  $pK_{as}$  of the fragments were good estimates for the ionisable groups of A $\beta$  peptides 1-40 and 1-42 by predicting separations in bare fused silica and poly(vinyl alcohol) (PVA) capillaries.

## 2. Materials and methods

### 2.1. Chemicals and reagents

All the chemicals used in the preparation of BGEs and solutions were of analytical reagent grade or better. Acetone, ammonia (25%), boric acid, diethylmalonic acid, hydrochloric acid (25%), methanol, phosphoric acid (85%), sodium acetate, potassium hydroxide, sodium dihydrogen phosphate, sodium formate and sodium hydroxide were supplied by Merck (Darmstadt, Germany). Tris(hydroxymethyl)aminomethane (Tris) was purchased from J.T. Baker (Deventer, Netherlands). Glutaraldehyde (50%) and PVA (hydrolysis grade 99%, average  $M_r$  90,000) were purchased from Sigma-Aldrich (Steinheim, Germany). Water with conductivity lower than  $0.05 \text{ Scm}^{-1}$  was obtained using a Milli-Q water purification system (Millipore, Molsheim, France). The fragments of A $\beta$  peptides 1-15, 10-20, 20-29, 25-35 and 33-42 and A $\beta$  peptides 1-40 and 1-42 were provided by Bachem (Bubendorf, Switzerland). Their sequences, ionisable groups and  $M_r$  are shown in Table 1.

### 2.2. Electrolyte solutions and samples solutions

The BGEs for the determination of  $m_e$  covered the pH range 2–12. They were prepared at the following concentrations (pH was adjusted with 1.0 M HCl or 1.0 M NaOH and

the I was calculated to be 25 mM): 15 mM NaH<sub>2</sub>PO<sub>4</sub> (pH 2.0), 25 mM NaH<sub>2</sub>PO<sub>4</sub> (pH 2.5–3.0), 25 mM sodium formate (pH 3.5–4.0), 25 mM sodium acetate (pH 4.5–5.0), 20 mM diethylmalonic acid (pH 5.5–6.5), 25 mM Tris (pH 7.0–9.0), 30 mM H<sub>3</sub>BO<sub>3</sub> (pH 9.5–10.5) and 5 mM H<sub>3</sub>PO<sub>4</sub> (pH 11.0–12.0). BGEs were passed through a 0.22 µm nylon filter (Panreac Applichem, Barcelona, Spain).

Individual stock solutions (1000 mg·L<sup>-1</sup>) of Aβ 1-15, 10-20, 20-29, 25-35 were prepared in water and Aβ 33-42 in 5 % (v/v) DMSO because it was less soluble in water. The working solutions (200 mg·L<sup>-1</sup>) contained 3% (v/v) acetone or 5 % (v/v) DMSO (Aβ 33-42) as electroosmotic flow (EOF) marker. A mixture of the five peptides (200 mg·L<sup>-1</sup>) was also prepared in water. Solvent and storage conditions were especially critical for Aβ 1-40 and 1-42, which were prone to aggregation. Aβ 1-40 and 1-42 were dissolved (1000 mg·L<sup>-1</sup>) in 50 mM and 100 mM ammonium hydroxide aqueous solutions, respectively, following the manufacturer's recommendation. A mixture of the two Aβ peptides (200 mg·L<sup>-1</sup>) was prepared in 100 mM ammonium hydroxide aqueous solution. All the stock solutions were divided into several aliquots and individually stored at -20 °C. Each aliquot was thawed only once, preserved in the refrigerator between injections and immediately discarded after the analyses.

### 2.3. Instrumental parameters

All CE-UV experiments were performed in an Agilent HP 3DCE system (Agilent Technologies, Waldbronn, Germany). Unless otherwise indicated, separations were performed at 25 °C in a 57 cm total length (L<sub>T</sub>) × 75 µm internal diameter (i.d.) × 365 µm outer diameter (o.d.) bare fused silica capillary (Polymicro Technologies, Phoenix,

AZ, USA). All capillary rinses were performed at high pressure (930 mbar). New capillaries were flushed with 1 M NaOH (15 min), water (15 min) and BGE (30 min). The system was finally equilibrated by applying 25 kV of separation voltage for 20 min (normal polarity, cathode in the outlet). Samples were injected at 50 mbar for 3 s. Between runs, capillaries were conditioned by rinsing with 1 M NaOH (1 min), water (1 min) and BGE (1 min). Between workdays or after a change of BGE, the capillary was conditioned by rinsing with 1 M NaOH (5 min), water (5 min) and BGE (10 min). The system was finally equilibrated by applying 25 kV of separation voltage for 20 min. Capillaries were stored overnight filled with water. For experiments with PVA capillaries, bare fused silica capillaries were coated with PVA following a procedure described elsewhere and cut to a  $L_T$  of 57 cm [26,27]. The conditioning, rinsing and separation methods were the same as in bare fused silica capillaries, but without using NaOH to prevent coating damage.

pH measurements were made with a Crison 2002 potentiometer and a Crison electrode 52-03 (Crison Instruments, Barcelona, Spain).

#### 2.4. Determination of electrophoretic mobility and acidity constants

The  $m_e$  of each A $\beta$  fragment was measured by CE-UV as the difference between the apparent mobility of each peptide,  $m_{app}$ , and the mobility of the neutral marker,  $m_{EOF}$  [15,18–21]:

$$m_e = m_{app} - m_{EOF} = \frac{L_C L_D}{V} \left( \frac{1}{t_{app}} - \frac{1}{t_{EOF}} \right) \quad (1)$$

Where  $L_C$  is the capillary length,  $L_D$  is the distance from the injection point to the detector and  $t_{app}$  and  $t_{EOF}$  are the migration time of the peptide and the neutral marker,

respectively. Individual solutions of each peptide were injected at each pH and  $m_e$  was obtained as the average of five replicates. BGEs indicated in Section 2.2 were run in sequence from low to high pH.

In previous studies [15,18–21] we established a general equation relating the  $m_e$  of a polyprotic substance  $H_nX^z$  ( $n$ =number of ionogenic groups and  $z$ =maximum net charge), to the pH of the BGE, taking into account the apparent  $pK_a$  values ( $pK_a'$ ) over the selected pH range. Table 2 shows the equation derived for each A $\beta$  fragment. It is worth mentioning that A $\beta$  1-15, 10-20 and 20-29 contained ionisable groups with equal or very similar  $pK_a'$  values, which were not possible to be separately determined by CE-UV ( $pK_a$  difference with Rickard et al. values [17] was less than 0.5 units, Table 3). Therefore, they were considered as a single group for ease of calculation (e.g. <sup>1</sup>C-Q and 2 D amino acids were combined in A $\beta$  1-15, Table 1, 2 and 3). Also note that acid-base equilibrium for the guanidine group in the R residue (Arg  $pK_a$  12.5 [17]) fell outside the studied pH range and was not considered for the calculations (Tables 1-3).

The  $pK_a'$  values were determined from nonlinear regression analysis of data pairs of  $m_e$ -pH (SciDAVis free software, 1.D009, Russell Standish, Sydney, Australia).

The effect of ionic strength ( $I$ ) upon  $pK_a'$  was taken into account, considering the activity coefficients of the solutes ( $\gamma$ ), obtained from the Guntelberg approximation of the extended law of Debye-Hückel (valid for  $I < 0.2$  M):

$$\log \gamma = \frac{-z^2 A \sqrt{I}}{1 + \sqrt{I}} \quad (2)$$

Where  $A$  is a temperature and solvent dielectric dependent constant with value of 0.509 in water at 25 °C.  $\gamma$  of neutral species ( $\gamma_0$ ) were assumed to be unity. Then, the thermodynamic  $pK_a$  values were easily calculated from the expression:

$$pK_{ai} = pK'_{ai} + \log \frac{\gamma^{z-(i-1)}}{\gamma^{z-i}} \quad (3)$$

The  $pK_{as}$  for A $\beta$  peptides 1-40 and 1-42 were estimated taking into account the thermodynamic  $pK_{as}$  obtained by CE-UV for the A $\beta$  fragments (Table 4).

## 2.5. Prediction of migration with the classical semiempirical models

In general, the  $m_e$  of a peptide is proportional to its  $q$  and inversely proportional to its Stoke's radius ( $r$ ). The  $r$  is generally expressed in terms of  $M_r$ , because the volume of a molecule is proportional to its mass if the density is constant [28,29]. The classical equations describing semiempirical models are deduced from assumptions concerning the peptide shapes and the forces that they undergo during electrophoretic motion. The general form of the equation relating  $m_e$ ,  $M_r$  and  $q$  is as follows:

$$m_e = B \frac{q}{M_r^\alpha} \quad (4)$$

where  $B$  is a constant and the parameter  $\alpha$  takes different values depending on the assumptions made on deduction of the semiempirical model ( $\alpha=1/2$ ,  $1/3$  and  $2/3$  for the classical polymer model, the Stoke's law and the Offord's surface law, respectively) [28,29].

In order to obtain  $q/M_r^\alpha$  values for the studied peptides,  $M_r$  was calculated from the amino acid sequences (Table 1) and  $q$  was calculated at each separation pH using the experimental CE-UV  $pK_{as}$  (Table 3) and Sillero and Ribeiro expression [30], which is based on the Henderson–Hasselbalch equation:

$$q = \sum_n \frac{P_n}{1+10^{pH-pK(P_n)}} - \sum_j \frac{N_j}{1+10^{pK(N_j)-pH}} \quad (5)$$

Where  $P_n$  and  $N_n$  are the cationic (i.e.  $P_1 =$  terminal  $\text{NH}_2$ ,  $P_2 = \text{H}$ ,  $P_3 = \text{K}$  and  $P_4 = \text{R}$ ) and anionic (i.e.  $N_1 =$  terminal  $\text{COOH}$ ,  $N_2 = \text{D}$ ,  $N_3 = \text{E}$  and  $N_4 = \text{Y}$ ) ionisable groups found in the amino acids, and  $\text{pK}_a(P_n)$  and  $\text{pK}_a(N_n)$  are the  $\text{pK}_a$ s of these groups. The accuracy of the  $q$  calculated in this way depends on the proposed sequence and the reliability of the  $\text{pK}_a$  considered for the ionisable groups [15]. Only for A $\beta$  1-15 (or later for A $\beta$  1-40 and 1-42), the average  $\text{pK}_a$  given by Rickard et al. [17] was used for the guanidine group in the R residue (12.5) because this  $\text{pK}_a$  could not be obtained by CE-UV (Tables 1-3).

Once linearity between  $m_e$  and  $q/M_r^\alpha$  was demonstrated for all the peptides at the different pH values,  $q/M_r^\alpha$  could be obtained at a certain pH to predict separation resolution or selectivity, as well as to simulate the electropherogram of a mixture, showing a pure Gaussian peak for each peptide [31]. As  $q/M_r^\alpha$  was inversely proportional to migration time,  $M_r^\alpha/q$  was considered for the graphic representations to show a correct migration order in the simulated electropherograms. In contrast to our previous works [18–21], now the influence of the EOF on migration time was also considered in the simulations:

$$h(x) = h_0 e^{-\frac{1}{2} \left[ \frac{x-x_i}{\sigma} \right]^2} \quad (6)$$

Where  $x$  corresponds to  $M_r^\alpha/q$  and defined the  $x$ -scale,  $h_0$  defined the peak height,  $\sigma$  was the standard deviation of the Gaussian peak ( $w_{1/2}$  (width at half height) =  $2.354 \cdot \sigma$ ) and  $x_i$  was related to the target peptide and the EOF at the studied pH value ( $M_{ri}^\alpha/q_i + 1/(C \cdot E)$ ) and it was the function value at the peak maximum for each peptide. The EOF influence at each pH value was taken into account adding the term  $1/(C \cdot E)$  in  $x_i$ , since the EOF was inversely related to migration time [32,33].  $C$  ranged between 0 and 1 and was the relative change of the EOF in a bare fused silica capillary at the studied pH

values. It was calculated as the ratio between the EOF mobility ( $m_{\text{EOF}}$ ) at the studied pH value and the maximum  $m_{\text{EOF}}$ , which corresponded in bare fused silica to pH 12. The curves of  $m_{\text{EOF}}$  variation as a function of pH were obtained from the literature [33].  $E$  was a constant to normalize the  $1/C$  values, in order to prevent the magnitude differences between  $1/C$  and  $M_{ri}^{\alpha}/q_i$ .  $E$  was arbitrarily selected as 1.1 times the most negative value of the  $M_{ri}^{\alpha}/q_i$  calculated for the peptides at the different pH values, in order to ensure simulation of all the negative ions because they migrated to the detector. For PVA capillaries, the same reasoning was applied and the curves of  $m_{\text{EOF}}$  variation as a function of pH were also obtained from the literature [34]. An average  $w_{1/2}$  value of 0.2 to calculate  $\sigma$  was fixed taking into account measurements of  $w_{1/2}$  in the experimental electropherograms. A value of 50 and 90 was arbitrarily selected as  $h_0$  for all the peptide peaks and for the EOF marker peak, respectively. In order to simplify the simulation procedure no other assumptions were made regarding peak shape or the influence of BGE composition on migration time and resolution. Microsoft Office Excel 2010 for Windows was used for all the calculations and simulations.

### 3. Results and discussion

#### 3.1. Electrophoretic behaviour and determination of $pK_a$ by CE-UV

The study of the electrophoretic behaviour of polyprotic compounds (e.g. peptides) as a function of pH can be simultaneously used for the accurate determination of their  $pK_a$ s and for selection of the optimum pH for separation of mixtures of the modelled compounds [15,18]. Figure 1 shows a plot of the experimental  $m_e$  for the studied A $\beta$  fragments (symbols) against the pH of the BGE. Good correlations were observed when

these experimental  $m_e$ -pH data pairs were fitted to the corresponding equations of Table 2 using nonlinear regression analysis (predicted  $m_e$ s are shown as solid curve lines,  $R^2 > 0.995$ ). Therefore, the proposed equations, which were deduced combining acid-base groups for some of the fragments (i.e. A $\beta$  1-15, 10-20 and 20-29), performed well despite the complexity of the polyprotic peptides and the approximations made to derive the equations for the different fragments (Tables 1 and 2). It is worth mentioning that when the electrophoretic models were modified in A $\beta$  1-15, 10-20 and 20-29 to consider all the non-equivalent ionisable groups separately (e.g. <sup>1</sup>C-Q and 2 D amino acids in A $\beta$  1-15, Table 1, 2 and 3), the calculation did not converge or the obtained  $pK_a$  values did not make chemical sense.

The thermodynamic  $pK_a$  of the peptides were calculated using the apparent  $pK'_a$  obtained from the best-fit parameters of each nonlinear regression model and are summarized in Table 3, together with the corresponding average  $pK_{a,s}$  given by Rickard et al. [17] and the  $pK_{a,s}$  of the free amino acids [35]. The average  $pK_{a,s}$  given by Rickard et al. were established for amino acids using the information collected for a large set of biosynthetic human insulin (BHI) and human growth hormone (hGH) short fragments with a few ionisable groups and are broadly used for proteins, polypeptides and small peptides studies. As can be seen, in general, the experimental  $pK_{a,s}$  obtained by CE-UV for the A $\beta$  fragments were very similar to the average  $pK_{a,s}$  given by Rickard et al., especially for the A $\beta$  25-35 and 33-42, which presented a lower number of ionisable groups. For the longer fragments, the most important shifts were found in the terminal ionisable carboxylic acid and amino groups, but not in the ionisable groups of the side chains. This effect was already observed by Rickard et al. when they compared their average  $pK_a$  values with the  $pK_a$  values for the free amino acids (Table 3) [17]. The

acidity of these terminal groups becomes weaker because the formation of the peptide bond induces an electrostatic change in the charge on the neighboring amino and carboxy groups. As the difference between our CE-UV  $pK_{as}$  and the average  $pK_{as}$  of Rickard et al. is very small, we recommend the use of these average  $pK_{as}$  for the amino acids when accurate  $pK_{as}$  for proteins and peptides are not available, for example, for electrophoretic separation prediction. These values are a far better approximation to the real  $pK_{as}$  than the  $pK_{as}$  of the free amino acids [15,18–20].

### 3.2. Classical semiempirical models for migration prediction.

The usefulness of equations in Table 2 for prediction of the electrophoretic behaviour of the studied peptides as a function of pH is limited because the number of experimental  $m_e$ -pH data pairs necessary for an accurate migration prediction is relatively large and increases with the number of ionisable groups. If accurate  $pK_a$  values are known (e.g. CE-UV  $pK_{as}$ ) or an appropriate estimation is available (e. g. Rickard et al.  $pK_{as}$  [17]), a better option to estimate a suitable pH for separation of the mixture is the approach based on the classic semiempirical relationships between  $m_e$  and  $q/M_r^\alpha$  [15,18–21]. Figure 2 shows for all the studied peptides in the pH range 2-12 the plot of  $m_e$  against  $q/M_r^\alpha$  for the classical polymer model ( $\alpha = 1/2$ ), the Stoke's law ( $\alpha = 1/3$ ) and the Offord's surface law ( $\alpha = 2/3$ ). In all cases, good linear correlations were observed ( $r^2 > 0.97$ ), confirming the validity of the classical semiempirical models in the whole pH range and the accuracy of the CE-UV  $pK_{as}$  used for charge calculation. The classical polymer model ( $r^2 \geq 0.978$ ) was considered for prediction of the separation of a mixture of the A $\beta$  fragments. This model was also the preferred model in our previous works to explain the migration behaviour of peptide hormones [15], neuropeptides [18],

apothioneins [19] and glycopeptides from tryptic digests of recombinant human erythropoietin [20].

Once the validity of the relationship between  $m_e$  and  $q/M_r^{1/2}$  is verified, a suitable pH for separation of the mixture can be estimated by selecting the appropriate pH to obtain the greatest differences between the curves of  $q/M_r^{1/2}$  vs pH for the A $\beta$  fragments. However, it is preferable to predict other parameters that quantitatively describe the extent of separation and the influence of the EOF. Predicting resolution ( $R_s$ ) between critically adjacent peaks is the best way to evaluate separation because efficiency and selectivity are simultaneously taken into account. In electrophoretic separations,  $R_s$  is usually calculated from the expression [32]:

$$R_s = \frac{\sqrt{N}}{4} \cdot \frac{(m_i - m_{i+1})}{(m_{avg} + m_{EOF})} \quad (7)$$

#### Efficiency Selectivity

Where  $N$  is the number of theoretical plates,  $m_i$  is the  $m_e$  of the peptides,  $m_{avg}$  is the average of  $m_i$  values and  $m_{EOF}$  is the EOF mobility. Resolution has been widely studied to optimise separations as a function of pH in CE with fused silica and coated capillaries [32,36]. If we suppose similar  $N$  values for all the peptides of the mixture, efficiency is considered as constant and only accounts for resolution the selectivity term. Furthermore, Equation 7 can be adapted to predict a parameter related to separation selectivity ( $S$ ) from the predicted  $q/M_r^{1/2}$ , taking into account the linear relationship between  $m_e$  and  $q/M_r^{1/2}$ :

$$S = \frac{(q/M_{ri}^{1/2} - q/M_{ri+1}^{1/2})}{(q/M_{r avg}^{1/2} + C * E)} \quad (8)$$

Where  $q/M_{ri}^{1/2}$  is the predicted  $q/M_r^{1/2}$  of the peptide  $i$ ,  $q/M_{r avg}^{1/2}$  is the average of  $q/M_{ri}^{1/2}$  values and  $C * E$  is the term taking into account the influence of the EOF at each pH value, as explained for equation 6 in section 2.5.

Equation 8 was used to predict  $S$  between adjacent peak pairs, considering the changes in migration orders that can be observed in Figure 1 and including the neutral marker peak, which migrates with the EOF ( $q/M_r^{1/2} = 0$ ). A plot of the predicted  $S$  between the worst-separated peak pair over the studied pH range permitted selection of the optimum pH for the separation of the five A $\beta$  fragments (Figure 3A). As observed in Figure 3A, the best separations were expected to be obtained at pH 3.0 and 10.5 because  $S$  was the highest. Separations were the worst in the pH range 5-9 because of the slight differences between  $q/M_r^{1/2}$  of the peptides or because they co-migrated with the EOF (their pIs were within that pH range, see Figure 1). In terms of selecting the optimum pH for the separation, this approach dramatically cuts down total optimisation time. Similar conclusions were drawn with an alternative quality criterion to optimise separations that Tascon et al. recently described [36], adapting  $t'$  to use  $q/M_r^{1/2}$  and considering the influence of the EOF.

$$t' = \frac{[q/M_{ri}^{1/2} * q/M_{ri+1}^{1/2} (q/M_{ri}^{1/2} - q/M_{ri+1}^{1/2})]^2}{C * E} \quad (9)$$

In this case, there was no need to consider the EOF peak to predict the separation from the neutrals but, as in  $S$  parameter, we introduced the term  $C * E$  in the denominator to take into account that separation decreases when EOF increases [32,33].

In order to further confirm the pH selection, the electropherograms for the separation of the mixture were simulated at pH 3.0 and 10.5 (Figure 3B and D). As can be observed, despite the simplicity of the approach, the agreement with the experimental electropherograms was good (Figure 3C and E). The mixture of the five A $\beta$  fragments was better resolved at acidic pH than at basic pH, where one of the peptides slightly

comigrated with the EOF. However, at pH 10.5 the total separation times were the lowest because the EOF in the fused silica capillary was much higher than at pH 3.0.

With regard to the A $\beta$  peptides 1-40 and 1-42, both contain a total of 15 ionisable groups corresponding to 8 different ionisable amino acids (Table 1). Once the accuracy of the experimental CE-UV pK<sub>a</sub>s of the A $\beta$  fragments was demonstrated predicting the electrophoretic behaviour and the selectivity of the separations, as well as simulating the electropherograms, these pK<sub>a</sub>s were used to estimate the pK<sub>a</sub>s of the 8 ionisable amino acids of the A $\beta$  peptides 1-40 and 1-42. An estimate of these pK<sub>a</sub>s was calculated as an average of the thermodynamic pK<sub>a</sub>s obtained by CE-UV for the A $\beta$  fragments (Table 4). As can be observed in Table 4, in most cases, the standard deviation of the pK<sub>a</sub>s of the A $\beta$  fragments used for the estimation was less than 0.2, hence justifying the validity of the approximation. Note in Table 4 that the average pK<sub>a</sub> given by Rickard et al. [17] was used as an estimate for the guanidine group in the R residue (12.5) of the A $\beta$  peptides 1-40 and 1-42 because this pK<sub>a</sub> could not be obtained by CE-UV for the fragments. The estimated pK<sub>a</sub>s of Table 4 were used to evaluate separations of A $\beta$  peptides 1-40 and 1-42. The plot of S between the A $\beta$  peptides over the pH range 2-12 allowed again a rapid selection of an appropriate pH for the separation (Figure 4A). As can be observed, the S values between the A $\beta$  1-40 and 1-42 were much smaller than before between the A $\beta$  fragments (compare the y-axis scale of Figure 3A and 4A). The best separation was predicted in the pH range 11.5-12. However, even at those conditions, S was very low, due to the very small structural differences between both peptides, which differ only in two amino acids that do not contain ionisable groups (Table 1). Figure 4B and C show the simulated and experimental electropherograms of the mixture at pH 11.5 in a fused silica capillary (fused silica is not very stable at pH

12.0). The simulation was in good agreement with the experimental results and, as expected, separation resolution was poor. The separation was also tested using 50  $\mu\text{m}$  and 30  $\mu\text{m}$  i.d bare fused silica capillaries, but resolution did not improve. Another interesting approach is the use of coated capillaries to control the EOF and to suppress analyte-wall interactions. Hydrophilic non-ionic coatings significantly reduce the EOF, suppress the adsorption of basic compounds to the capillary wall and, in some cases, could act as a pseudo-stationary phase. Among these, permanently coated hydroxypropyl cellulose (HPC) and PVA capillaries have proven to exhibit a particularly good performance in terms of stability and reproducibility [26,27,37,38]. In our case, only PVA capillaries gave remarkable results with regard to separations of A $\beta$  1-40 and 1-42 peptides. In order to ensure the stability of the coating, separation was done at pH 10.0 instead of pH 11.5 (Figure 4A). Figs. 4D and E show that again concordance between the simulated and experimental electropherograms is good, because the EOF magnitude is taken into account for the simulations [34]. Furthermore, the EOF reduction at pH 10.0 in PVA capillaries, with regard to a fused silica capillary at pH 11.5 (more than 40% in our case), allowed a slight improvement of the resolution between both peptides, at the expense of a slight increase in total separation time. In order to further improve this separation, it would be necessary to explore complementary mechanisms based on interactions with a pseudo-stationary phase, a complexing agent or to use on-line MS detection.

#### 4. Concluding remarks

In this study, we have estimated by CE-UV the pK<sub>a</sub>s of A $\beta$  peptides 1-40 and 1-42 from five A $\beta$  peptide fragments covering all their complete amino acid sequence. First, the experimental m<sub>e</sub>s of the five fragments in the studied pH range were fitted to equations

modelling their ionisable behaviour as a function of pH. The accuracy of the pK<sub>a</sub>s was demonstrated predicting the electrophoretic behaviour of the studied fragments and separation selectivity of their mixture using the classical polymer model. Bearing in mind the excellent results and the simplicity of the approach, if accurate pK<sub>a</sub> values are available for the target compounds, this is a remarkable strategy for making a rapid and “dry” selection of the optimum pH for the separation of their mixtures. The pK<sub>a</sub>s of the fragments were also valuable estimates for the Aβ 1-40 and 1-42 (<sup>1</sup>C and D 3.1, E 4.6 and Y 10.8 for acidic amino acids and <sup>1</sup>N-D 8.6, H 6.0, K 10.6 and R 12.5 for basic amino acids). Therefore, the estimation of pK<sub>a</sub>s of complex polyprotic peptides from their building peptide fragments can be regarded as a straightforward and reliable method to acquire information that could not be readily acquired by other means.

### **Acknowledgements**

This study was supported by a grant from the Spanish Ministry of Economy and Competitiveness (CTQ2014-56777-R). Roger Però-Gascón acknowledges the Generalitat de Catalunya for a FI-DGR fellowship. We also thank Lleonart Quiles for his collaboration in part of this study.

**References**

- [1] S.K. Poole, S. Patel, K. Dehring, H. Workman, C.F. Poole, Determination of acid dissociation constants by capillary electrophoresis, *J. Chromatogr. A.* 1037 (2004) 445–454. doi:10.1016/j.chroma.2004.02.087.
- [2] S. Babić, A.J.M. Horvat, D. Mutavdžić Pavlović, M. Kaštelan-Macan, Determination of pKa values of active pharmaceutical ingredients, *TrAC - Trends Anal. Chem.* 26 (2007) 1043–1061. doi:10.1016/j.trac.2007.09.004.
- [3] P. Nowak, M. Wozniakiewicz, P. Koscielniak, Application of capillary electrophoresis in determination of acid dissociation constant values, *J. Chromatogr. A.* 1377 (2015) 1–12. doi:10.1016/j.chroma.2014.12.032.
- [4] R. Konášová, J.J. Dyrťová, V. Kašička, Determination of acid dissociation constants of triazole fungicides by pressure assisted capillary electrophoresis., *J. Chromatogr. A.* 1408 (2015) 243–249. doi:10.1016/j.chroma.2015.07.005.
- [5] Z. Qiang, C. Adams, Potentiometric determination of acid dissociation constants (pKa) for human and veterinary antibiotics, *Water Res.* 38 (2004) 2874–2890. doi:10.1016/j.watres.2004.03.017.
- [6] R.I. Allen, K.J. Box, J.E.A. Comer, C. Peake, K.Y. Tam, Multiwavelength spectrophotometric determination of acid dissociation constants of ionizable drugs, *J. Pharm. Biomed. Anal.* 17 (1998) 699–712. doi:10.1016/S0731-7085(98)00010-7.
- [7] J. Bezençon, M.B. Wittwer, B. Cutting, M. Smieško, B. Wagner, M. Kansy, B. Ernst, pKa determination by <sup>1</sup>H NMR spectroscopy - An old methodology revisited, *J. Pharm. Biomed. Anal.* 93 (2014) 147–155. doi:10.1016/j.jpba.2013.12.014.
- [8] J. Barbosa, D. Barrón, E. Jiménez-Lozano, V. Sanz-Nebot, Comparison between

- capillary electrophoresis, liquid chromatography, potentiometric and spectrophotometric techniques for evaluation of pK<sub>a</sub> values of zwitterionic drugs in acetonitrile-water mixtures, *Anal. Chim. Acta.* 437 (2001) 309–321. doi:10.1016/S0003-2670(01)00997-7.
- [9] S. Ehala, J. Míšek, I.G. Stará, I. Starý, V. Kašička, Determination of acid-base dissociation constants of azahelicenes by capillary zone electrophoresis, *J. Sep. Sci.* 31 (2008) 2686–2693. doi:10.1002/jssc.200800227.
- [10] M. Shalaeva, J. Kenseth, F. Lombardo, A. Bastin, Measurement of dissociation constants (pK<sub>a</sub> values) of organic compounds by multiplexed capillary electrophoresis using aqueous and cosolvent buffers, *J. Pharm. Sci.* 97 (2008) 2581–2606. doi:10.1002/jps.21287.
- [11] C.A. Currie, W.R. Heineman, H.B. Halsall, C.J. Seliskar, P.A. Limbach, F. Arias, K.R. Wehmeyer, Estimation of pK<sub>a</sub> values using microchip capillary electrophoresis and indirect fluorescence detection, *J. Chromatogr. B Anal. Technol. Biomed. Life Sci.* 824 (2005) 201–205. doi:10.1016/j.jchromb.2005.07.035.
- [12] X. Fu, Y. Liu, W. Li, Y. Bai, Y. Liao, H. Liu, Determination of dissociation constants of aristolochic acid I and II by capillary electrophoresis with carboxymethyl chitosan-coated capillary, *Talanta.* 85 (2011) 813–815. doi:10.1016/j.talanta.2011.03.088.
- [13] G. Aptisa, F. Benavente, V. Sanz-Nebot, E. Chirila, J. Barbosa, Evaluation of migration behaviour of therapeutic peptide hormones in capillary electrophoresis using polybrene-coated capillaries, *Anal. Bioanal. Chem.* 396 (2010) 1571–1579. doi:10.1007/s00216-009-3344-1.
- [14] H. Wan, A.G. Holmén, Y. Wang, W. Lindberg, M. Englund, M.B. Någård, R.A.

- Thompson, High-throughput screening of pKa values of pharmaceuticals by pressure-assisted capillary electrophoresis and mass spectrometry, *Rapid Commun. Mass Spectrom.* 17 (2003) 2639–2648. doi:10.1002/rcm.1229.
- [15] F. Benavente, E. Balaguer, J. Barbosa, V. Sanz-Nebot, Modelling migration behavior of peptide hormones in capillary electrophoresis-electrospray mass spectrometry, *J. Chromatogr. A.* 1117 (2006) 94–102. doi:10.1016/j.chroma.2006.03.049.
- [16] J.M. Cabot, E. Fuguet, M. Rosés, P. Smejkal, M.C. Breadmore, Novel instrument for automated pKa determination by internal standard capillary electrophoresis, *Anal. Chem.* 87 (2015) 6165–6172. doi:10.1021/acs.analchem.5b00845.
- [17] E.C. Rickard, M.M. Strohl, R.G. Nielsen, Correlation of electrophoretic mobilities from capillary electrophoresis with physicochemical properties of proteins and peptides, *Anal. Biochem.* 197 (1991) 197–207. doi:10.1016/0003-2697(91)90379-8.
- [18] V. Sanz-Nebot, F. Benavente, E. Hernández, J. Barbosa, Evaluation of the electrophoretic behaviour of opioid peptides. Separation by capillary electrophoresis-electrospray ionization mass spectrometry, *Anal. Chim. Acta.* 577 (2006) 68–76. doi:10.1016/j.aca.2006.06.035.
- [19] F. Benavente, B. Andón, E. Giménez, J. Barbosa, V. Sanz-Nebot, Modeling the migration behavior of rabbit liver apothioneins in capillary electrophoresis, *Electrophoresis.* 29 (2008) 2790–2800. doi:10.1002/elps.200700852.
- [20] A. Barroso, E. Gimenez, F. Benavente, J. Barbosa, V. Sanz-Nebot, Modelling the electrophoretic migration behaviour of peptides and glycopeptides from glycoprotein digests in capillary electrophoresis-mass spectrometry, *Anal. Chim. Acta.* 854 (2015) 169–177. doi:10.1016/j.aca.2014.10.038.

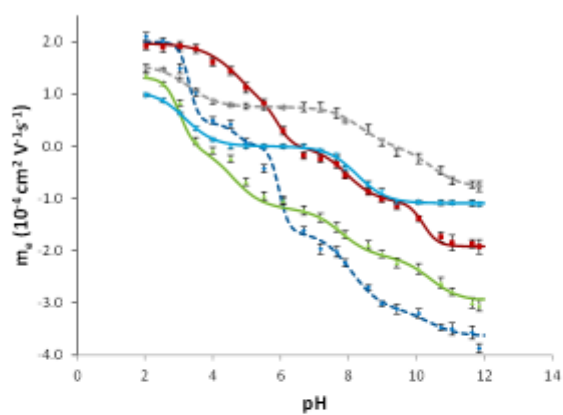
- [21] F. Benavente, E. Giménez, D. Barrón, J. Barbosa, V. Sanz-Nebot, Modeling the electrophoretic behavior of quinolones in aqueous and hydroorganic media, *Electrophoresis*. 31 (2010) 965–972. doi:10.1002/elps.200900344.
- [22] S. Sabella, M. Quaglia, C. Lanni, M. Racchi, S. Govoni, G. Caccialanza, A. Calligaro, V. Bellotti, E. De Lorenzi, Capillary electrophoresis studies on the aggregation process of beta-amyloid 1-42 and 1-40 peptides., *Electrophoresis*. 25 (2004) 3186–3194. doi:10.1002/elps.200406062.
- [23] N.E. Pryor, M.A. Moss, C.N. Hestekin, Capillary electrophoresis for the analysis of the effect of sample preparation on early stages of A $\beta$ (1-40) aggregation, *Electrophoresis*. 35 (2014) 1814–1820. doi:10.1002/elps.201400012.
- [24] D. Bhowmik, C.M. MacLaughlin, M. Chandrakesan, P. Ramesh, R. Venkatramani, G.C. Walker, S. Maiti, pH changes the aggregation propensity of amyloid- $\beta$  without altering the monomer conformation., *Phys. Chem. Chem. Phys.* 16 (2014) 885–889. doi:10.1039/c3cp54151g.
- [25] S. Kobayashi, Y. Tanaka, M. Kiyono, M. Chino, T. Chikuma, K. Hoshi, H. Ikeshima, Dependence pH and proposed mechanism for aggregation of Alzheimer's disease-related amyloid-B (1-42) protein, *J. Mol. Struct.* 1094 (2015) 109–117. doi:10.1016/j.molstruc.2015.03.023.
- [26] M. Gilges, M.H. Kleemiss, G. Schomburg, Capillary zone electrophoresis separations of basic and acidic proteins using poly(vinyl alcohol) coatings in fused silica capillaries, *Anal. Chem.* 66 (1994) 2038–2046. doi:10.1021/ac00085a019.
- [27] Y. Shen, R.D. Smith, High-resolution capillary isoelectric focusing of proteins using highly hydrophilic-substituted cellulose-coated capillaries, *J. Microcolumn Sep.* 12 (2000) 135–141. doi:10.1002/(SICI)1520-667X(2000)12:3<135::AID-

- MCS2>3.0.CO;2-5.
- [28] N.J. Adamson, E.C. Reynolds, Rules relating electrophoretic mobility, charge and molecular size of peptides and proteins, *J. Chromatogr. B Biomed. Appl.* 699 (1997) 133–147. doi:10.1016/S0378-4347(97)00202-8.
- [29] A. Cifuentes, H. Poppe, Behavior of peptides in capillary electrophoresis: Effect of peptide charge, mass and structure, *Electrophoresis*. 18 (1997) 2362–2376. doi:10.1002/elps.1150181227.
- [30] A. Sillero, J.M. Ribeiro, Isoelectric points of proteins: Theoretical determination, *Anal. Biochem.* 179 (1989) 319–325. doi:10.1016/0003-2697(89)90136-X.
- [31] J.R. Torres-Lapasió, J.J. Baeza-Baeza, M.C. García-Alvarez-Coque, A model for the description, simulation, and deconvolution of skewed chromatographic peaks, *Anal. Chem.* 69 (1997) 3822–3831. doi:10.1021/ac970223g.
- [32] J.W. Jorgenson, K.D. Lukacs, Zone electrophoresis in open-tubular glass capillaries, *Anal. Chem.* 53 (1981) 1298–1302. doi:10.1002/jhrc.1240040507.
- [33] K.D. Lukacs, J.W. Jorgenson, Capillary zone electrophoresis: Effect of physical parameters on separation efficiency and quantitation, *J. High Resol. Chromatogr.* 8 (1985) 407–411. doi:10.1002/jhrc.1240080810.
- [34] M. Poitevin, A. Morin, J.M. Busnel, S. Descroix, M.C. Hennion, G. Peltre, Comparison of different capillary isoelectric focusing methods-use of “narrow pH cuts” of carrier ampholytes as original tools to improve resolution, *J. Chromatogr. A*. 1155 (2007) 230–236. doi:10.1016/j.chroma.2007.02.013.
- [35] D.L. Nelson, M.M. Cox, *Lehninger Principles of Biochemistry*, 5th ed., W. H. Freeman, New York, 2008.
- [36] M. Tascon, F. Benavente, C.B. Castells, L.G. Gagliardi, Quality criterion to optimize separations in capillary electrophoresis : Application to the analysis of

- harmala alkaloids, *J. Chromatogr. A.* 1460 (2016) 190–196. doi:10.1016/j.chroma.2016.07.032.
- [37] D. Belder, A. Deege, H. Husmann, F. Kohler, M. Ludwig, Cross-linked poly(vinyl alcohol) as permanent hydrophilic column coating for capillary electrophoresis, *Electrophoresis.* 22 (2001) 3813–3818. doi:10.1002/1522-2683(200109)22:17<3813::AID-ELPS3813>3.0.CO;2-D.
- [38] G.G. Wolken, E.A. Arriaga, Simultaneous measurement of individual mitochondrial membrane potential and electrophoretic mobility by capillary electrophoresis, *Anal. Chem.* 86 (2014) 4217–4226. doi:10.1021/ac403849x.

**Figure legends**

**Figure 1.** Experimental (symbols) and predicted (lines)  $m_e$  vs. pH of the BGEs for A $\beta$  fragments 1-15 ( $\blacklozenge$ ), 10-20 ( $\blacksquare$ ), 20-29 ( $\blacktriangle$ ), 25-35 (X) and 33-42 ( $\blacktimes$ ). The error bars show standard deviations (n=5).

**Figure 1**

**Figure 2.** Correlation between  $m_e$  and  $q/M_r^\alpha$  for the A $\beta$  fragments in the pH range 2–12.  $\alpha = 1/2$ ,  $1/3$  and  $2/3$  for the classical polymer model, the Stoke's law and the Offord's surface law, respectively. ( $q/M_r^\alpha$  values were calculated with the experimental CE-UV pK<sub>a</sub>s, excepting for the guanidine group in the R residue in A $\beta$  1-15 [17] (Table 3)).

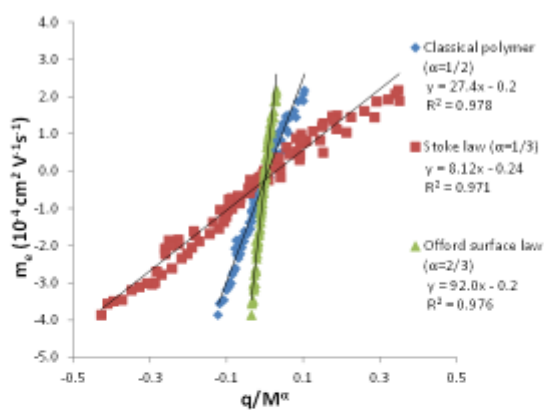


**Figure 2**

**Figure 3.** A) Selectivity (S) of the worst-separated peak pair in a mixture of the five A $\beta$  fragments in the pH range 2-12. Simulated and experimental electropherograms of a mixture of the five A $\beta$  fragments at pH 3.0 (B and C) and 10.5 (D and E).

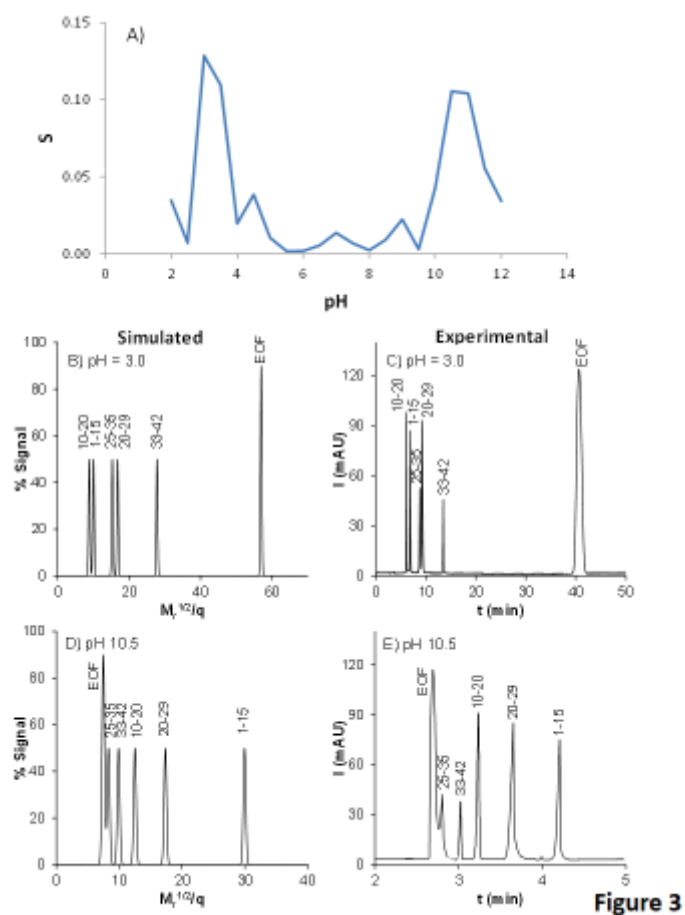


**Figure 3**

**Figure 4.** A) Selectivity ( $S$ ) between the A $\beta$  1-40 and 1-42 peptides in the pH range 2-12 in a bare fused silica capillary (solid line) and in the pH range 2-10 in a PVA coated capillary (dash line). ( $q/M_r^{1/2}$  values were calculated with the estimated pK<sub>a</sub>s of the A $\beta$  peptides 1-40 and 1-42, excepting for the guanidine group in the R residue [17] (Table 4)). Simulated and experimental electropherograms of a mixture of A $\beta$  1-40 and 1-42 peptides at pH 11.5 (bare fused silica capillary) (B and C) and 10.0 (PVA coated capillary) (D and E).

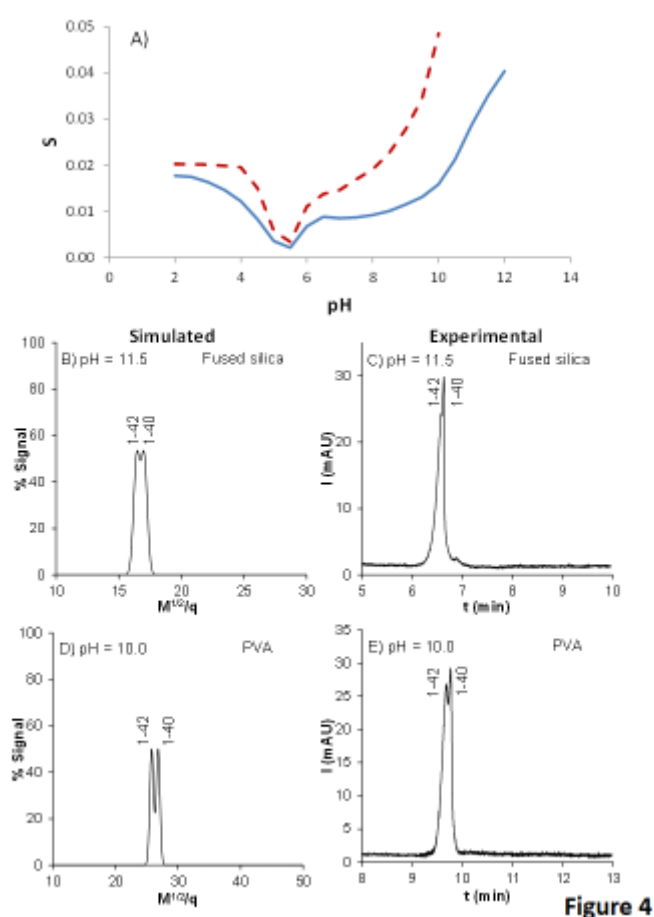


**Figure 4**

**Table 1.** Amino acid sequence, relative monoisotopic molecular mass ( $M_r$ ) and ionisable groups for the studied A $\beta$  peptides.

A $\beta$ peptide sequence	$M_r$	Ionisable amino acids		Formula	
		Aci dic <sup>a</sup>	Bas ic <sup>b</sup>	$H_aABH$	$H_nX^z$
<b>1-15</b> DAEFRHDSGYEVHHQ	182 6.9	1 <sup>13</sup> C- Q c1 2 D c1 2 E c2 1 Y	1 <sup>14</sup> N- D 3 H c3 1 R d	$H_6ABH$	$H_{11}X_{5+}$
<b>10-20</b> YEVHHQKLVFF	144 6.7	1 <sup>13</sup> C- F 1 E 1 Y e2	1 <sup>14</sup> N- Y 2 H e1 1 K e2	$H_3ABH$	$H_7X_4^+$
<b>20-29</b> FAEDVGSNKG	102 3.1	1 <sup>13</sup> C- G <sup>f</sup> 1 D <sup>f</sup> 1 E	1 <sup>14</sup> N- F 1 K	$H_3ABH$	$H_5X_2^+$
<b>25-35</b> GSNKGAIIGLM	106 0.3	1 <sup>13</sup> C- M	1 <sup>14</sup> N- G 1 K	$HABH_2$	$H_3X_2^+$
<b>33-42</b> GLMVGGVVIA	915. 2	1 <sup>13</sup> C- A	1 <sup>14</sup> N- G	$HABH^+$	$H_2X^+$
<b>1-40</b> DAEFRHDSGYEVHHQKLVFFAEDVGSNKGAIIGLMVGGVVV	432 9.9	1 <sup>13</sup> C- V 3 D 3	1 <sup>14</sup> N- D 3 H 2 K 1 R	$H_8ABH$	$H_{15}X_{7+}$

		E 1 Y		
<b>1-42</b> <b>DAEFRHDSGYEVHHQKLVFFAEDVGSNK</b> <b>GAIIGLMVGGVVIA</b>	451 4.1	1 'C- A 3 D 3 E 1 Y	1 'N- D 3 H 2 K 1 R	<b>H<sub>8</sub>ABH<sub>7</sub><sup>+</sup></b> H <sub>15</sub> X <sub>7<sup>+</sup></sub>

a) In this column 'C-: Terminal COOH.

b) In this column 'N-: Terminal NH<sub>2</sub>.

The following ionisable groups were combined for the calculations:

c1) 1 'C-Q and 2 D

c2) 2 E

c3) 3 H

e1) 2 H

e2) 1 Y and 1 K

f) 1 'C-G and 1 D

d) R was not considered for the calculations because the expected pK<sub>a</sub> was outside the studied pH range (2-12).

**Table 2.** Electrophoretic models for the studied A $\beta$  fragments in the pH range 2-12.

A $\beta$ Fragment	H <sub>n</sub> X <sup>z</sup>	Electrophoretic model
1-15 <sup>a, b</sup>	H <sub>11</sub> X <sup>5+</sup>	$m_e = \frac{10^{(3pK'_1+2pK'_2-5pH)}m_{H_{11}X^{5+}} + 10^{(2pK'_2-2pH)}m_{H_8X^{2+}} + 10^{(3pH-3pK'_3)}m_{H_3X^{3-}} + 10^{(4pH-3pK'_3-pK'_4)}m_{H_2X^{4-}} + 10^{(5pH-3pK'_3-pK'_4-pK'_5)}m_{H_1X^{5-}}}{10^{(3pK'_1+2pK'_2-5pH)} + 10^{(2pK'_2-2pH)} + 1 + 10^{(3pH-3pK'_3)} + 10^{(4pH-3pK'_3-pK'_4)} + 10^{(5pH-3pK'_3-pK'_4-pK'_5)}}$
10-20 <sup>c</sup>	H <sub>7</sub> X <sup>4+</sup>	$m_e = \frac{10^{(pK'_1+pK'_2+2pK'_3-4pH)}m_{H_7X^{4+}} + 10^{(pK'_2+2pK'_3-3pH)}m_{H_6X^{3+}} + 10^{(2pK'_3-2pH)}m_{H_5X^{2+}} + 10^{(pH-pK'_4)}m_{H_2X^{-}} + 10^{(3pH-pK'_4-pK'_5)}m_{H_1X^{3-}}}{10^{(pK'_1+pK'_2+2pK'_3-4pH)} + 10^{(pK'_2+2pK'_3-3pH)} + 10^{(2pK'_3-2pH)} + 1 + 10^{(pH-pK'_4)} + 10^{(3pH-pK'_4-pK'_5)}}$
20-29 <sup>d</sup>	H <sub>5</sub> X <sup>2+</sup>	$m_e = \frac{10^{(2pK'_1-2pH)}m_{H_5X^{2+}} + 10^{(pH-pK'_2)}m_{H_2X^{-}} + 10^{(2pH-pK'_2-pK'_3)}m_{HX^{2-}} + 10^{(3pH-pK'_2-pK'_3-pK'_4)}m_{X^{3-}}}{10^{(2pK'_1-2pH)} + 1 + 10^{(pH-pK'_2)} + 10^{(2pH-pK'_2-pK'_3)} + 10^{(3pH-pK'_2-pK'_3-pK'_4)}}$
25-35	H <sub>3</sub> X <sup>2+</sup>	$m_e = \frac{10^{(pK'_1+pK'_2-2pH)}m_{H_3X^{2+}} + 10^{(pK'_2-pH)}m_{H_2X^{+}} + 10^{(pH-pK'_3)}m_{X^{-}}}{10^{(pK'_1+pK'_2-2pH)} + 10^{(pK'_2-pH)} + 1 + 10^{(pH-pK'_3)}}$
33-42	H <sub>2</sub> X <sup>+</sup>	$m_e = \frac{10^{(pK'_1-pH)}m_{H_2X^{+}} + 10^{(pH-pK'_2)}m_{X^{-}}}{10^{(pK'_1-pH)} + 1 + 10^{(pH-pK'_2)}}$

a) R (Arg) was not considered for the calculations because the expected pK<sub>a</sub> was outside the studied pH range (2-12).

The ionisable groups of the following amino acids were combined for the calculations because the pK<sub>a</sub> values were expected similar:

- b) 1 'C-Q and 2D (pK'<sub>1</sub>), 2 E (pK'<sub>2</sub>), 3 H (pK'<sub>3</sub>).
- c) 2H (pK'<sub>3</sub>), 1 Y and 1 K (pK'<sub>5</sub>).
- d) 1 'C-G and 1 D (pK'<sub>1</sub>).

**Table 3.** CE-UV apparent  $pK_{as}$  ( $pK'_a$ ), thermodynamic  $pK_{as}$ ,  $pK_{as}$  of Rickard et al. [17] and  $pK_{as}$  of the free amino acid [35].

A $\beta$ fragment	$pK'_a$	$pK'_i$	$\gamma_i/\gamma_j$	$pK_a$	$pK_a$ Rickard et al.	$pK_a$ free amino acid	Amino acid <sup>a</sup>
<b>1-15</b>	3.5 $\pm$ 0.3 <sup>b1</sup>	<b>1</b>	$\gamma_{5+}/\gamma_{4+}$	<b>2.9</b>	3.2	<b>2.2</b>	<sup>13</sup> C-Q
			$\gamma_{4+}/\gamma_{3+}$	<b>3.0</b>	3.5	<b>3.7</b>	D
			$\gamma_{3+}/\gamma_{2+}$	<b>3.1</b>	3.5	<b>3.7</b>	D
	4.7 $\pm$ 0.7 <sup>b2</sup>	<b>2</b>	$\gamma_{2+}/\gamma_+$	<b>4.5</b>	4.5	<b>4.3</b>	E
			$\gamma_+/\gamma_0$	<b>4.6</b>	4.5	<b>4.3</b>	E
			$\gamma_0/\gamma_-$	<b>6.0</b>	6.2	<b>6.0</b>	H
	6.0 $\pm$ 0.1 <sup>b3</sup>	<b>3</b>	$\gamma_-/\gamma_{2-}$	<b>6.2</b>	6.2	<b>6.0</b>	H
			$\gamma_{2-}/\gamma_{3-}$	<b>6.3</b>	6.2	<b>6.0</b>	H
			$\gamma_{3-}/\gamma_{4-}$	<b>8.6</b>	8.6	<b>9.6</b>	<sup>15</sup> N-D
	8.1 $\pm$ 0.4	<b>4</b>	$\gamma_{4-}/\gamma_{5-}$	<b>11.1</b>	10.3	<b>10.1</b>	Y
10.4 $\pm$ 0.7	<b>5</b>	$\gamma_{5-}/\gamma_{6-}$	-	12.5	<b>12.5</b>	R	
- <sup>c</sup>	-						
<b>10-20</b>	3.8 $\pm$ 0.2	<b>1</b>	$\gamma_{4+}/\gamma_{3+}$	<b>3.3</b>	3.2	<b>1.8</b>	<sup>13</sup> C-F
	4.9 $\pm$ 0.6	<b>2</b>	$\gamma_{3+}/\gamma_{2+}$	<b>4.5</b>	4.5	<b>4.3</b>	E
	6.0 $\pm$ 0.2 <sup>d1</sup>	<b>3</b>	$\gamma_{2+}/\gamma_+$	<b>5.7</b>	6.2	<b>6.0</b>	H
			$\gamma_+/\gamma_0$	<b>5.9</b>	6.2	<b>6.0</b>	H
	8.0 $\pm$ 0.1	<b>4</b>	$\gamma_0/\gamma_-$	<b>8.0</b>	7.7	<b>9.1</b>	<sup>15</sup> N-Y
	10.2 $\pm$ 0.1 <sup>d2</sup>	<b>5</b>	$\gamma_-/\gamma_{2-}$	<b>10.4</b>	10.3	<b>10.1</b>	Y
			$\gamma_{2-}/\gamma_{3-}$	<b>10.6</b>	10.3	<b>10.5</b>	K
<b>20-29</b>	3.2 $\pm$ 0.1 <sup>e</sup>	<b>1</b>	$\gamma_{2+}/\gamma_+$	<b>2.9</b>	3.2	<b>2.3</b>	<sup>13</sup> C-G
			$\gamma_+/\gamma_0$	<b>3.1</b>	3.5	<b>3.7</b>	D
	4.6 $\pm$ 0.1	<b>2</b>	$\gamma_0/\gamma_-$	<b>4.7</b>	4.5	<b>4.3</b>	E
	7.8 $\pm$ 0.2	<b>3</b>	$\gamma_-/\gamma_{2-}$	<b>8.1</b>	7.7	<b>9.1</b>	<sup>15</sup> N-F
	10.5 $\pm$ 0.2	<b>4</b>	$\gamma_{2-}/\gamma_{3-}$	<b>10.8</b>	10.3	<b>10.5</b>	K
<b>25-35</b>	3.3 $\pm$ 0.1	<b>1</b>	$\gamma_{2+}/\gamma_+$	<b>3.1</b>	3.2	<b>2.3</b>	<sup>13</sup> C-M
	8.3 $\pm$ 0.1	<b>2</b>	$\gamma_+/\gamma_0$	<b>8.2</b>	8.2	<b>9.6</b>	<sup>15</sup> N-G
	10.5 $\pm$ 0.1	<b>3</b>	$\gamma_0/\gamma_-$	<b>10.5</b>	10.3	<b>10.5</b>	K
<b>33-42</b>	3.2 $\pm$ 0.1	<b>1</b>	$\gamma_+/\gamma_0$	<b>3.1</b>	3.2	<b>2.3</b>	<sup>13</sup> C-A
	8.3 $\pm$ 0.1	<b>2</b>	$\gamma_0/\gamma_-$	<b>8.3</b>	8.2	<b>9.6</b>	<sup>15</sup> N-G

a) <sup>13</sup>C-: Terminal COOH; <sup>15</sup>N-: Terminal NH<sub>2</sub>.

c) R (Arg) was not considered for the calculations because the expected  $pK_a$  was outside the studied pH range (2-12).

b1, b2, b3, c1, c2 and d) The ionisable groups were combined for the calculations (See Table 1).

**Table 4.** Thermodynamic pK<sub>a</sub>s for Aβ fragments obtained by CE (from Table 3) and average pK<sub>a</sub>s calculated as an estimate of the pK<sub>a</sub>s of Aβ peptides 1-40 and 1-42.

Ionisable amino acid <sup>a</sup>	Aβ fragment	pK <sub>a</sub> <sup>b</sup>	Average pK <sub>a</sub>	Standard deviation	Number of residues in the sequence of the Aβ peptide	
					1-40	1-42
<sup>13</sup> C	1-15	<b>2.9 (Q)</b>	3.1	<b>0.2</b>	1 (V)	1 (A)
	10-20	<b>3.3 (F)</b>				
	20-29	<b>2.9 (G)</b>				
	25-35	<b>3.1 (M)</b>				
	33-42	<b>3.1 (A)</b>				
D	1-15	<b>3.0</b> <b>3.1</b>	3.1	<b>0.1</b>	3	3
	10-20	<b>3.1</b>				
E	1-15	<b>4.5</b> <b>4.6</b> <sup>c1</sup>	4.6	<b>0.1</b>	3	3
	10-20	<b>4.5</b> <sup>c1</sup>				
	20-29	<b>4.7</b>				
H	1-15	<b>6.0</b> <b>6.2</b> <sup>d1</sup> <b>6.3</b> <sup>d2</sup>	6.0	<b>0.1</b>	3	3
	10-20	<b>5.7</b> <sup>d1</sup> <b>5.9</b> <sup>d2</sup>				
<sup>15</sup> N	1-15	<b>8.6 (D)</b>	8.6	-	1 (D)	1 (D)
K	10-20	<b>10.6</b>	10.6	<b>0.2</b>	2	2
	20-29	<b>10.8</b> <sup>e1</sup>				
	25-35	<b>10.5</b> <sup>e1</sup>				
Y	1-15	<b>11.1</b>	10.8	<b>0.5</b>	1	1
	10-20	<b>10.4</b>				
R	1-15	- <sup>f</sup>	12.5 <sup>g</sup>	-	1	1

a) <sup>13</sup>C: Terminal COOH; <sup>15</sup>N: Terminal NH<sub>2</sub>. The terminal amino acids are indicated between parentheses.

b) Experimental CE-UV thermodynamic pK<sub>a</sub>s for Aβ fragments (See Table 3).

c1, d1, d2 and e1) The same position of the amino acid sequence is repeated in both Aβ fragments.

f) pK<sub>a</sub> of R (Arg) was not determined by CE-UV because the expected pK<sub>a</sub> was outside the studied pH range (2-12).

g) pK<sub>a</sub> of R (Arg) of Rickard et al. [17].